35th International Electric Vehicle Symposium and Exhibition (EVS35)
Oslo, Norway, June 11-15, 2022

Development of a Square-Wave Voltage Source for Laboratory Tests of Inductive Power Transmission

Daniel Barth[1], Johannes Scholl, Michael Stahl, Erik Wöhr,
Michael Suriyah, Thomas Leibfried
[1]*Karlsruhe Institute of Technology (KIT), Karlsruhe, Germany. E-mail: daniel.barth@kit.edu*

Executive Summary

This publication describes the concept and implementation of a voltage-source converter for laboratory tests of inductive wireless power transmission (WPT). The power electronics, the measurement systems, the safety technology and the software for controlling the converter are discussed. The converter can be operated on the three-phase low-voltage grid and outputs a square-wave voltage with a frequency of up to 100 kHz. The output power is limited by the mains connection power at 400 V and 63 A. In addition to the converter concept, the content focuses on experience gained during commissioning. Encountered problems, approaches to solutions and useful features are described in this work.

Keywords: inductive charger, testing processes, semi-conductor, converter, controller

1 Introduction

Research on inductive charging systems for electric vehicles requires a suitable test environment. Coil design, control and electrical metrology can only be evaluated in tests if an inverter platform equipped for this purpose is available.
With the ongoing development and standardization of inductive charging, the topology of the full-bridge inverter as a square-wave voltage source has become established. Examples of this topology include the reference systems in [1]. In principle, numerous topologies are suitable for the implementation of the inverter. Both voltage-fed and current-fed inverters are possible, as is the use of one or more half-bridges and different power semiconductor components. Comparisons of different options can be found in [2], among others. Self-oscillating concepts are also possible [3, 4].
We focus on the voltage-fed full-bridge inverter. In order to test high-power WPT, the power requirements, the frequency band in the range of 79 kHz to 90 kHz [1] and especially the programmability preclude a commercially available solution. In the academic context, a commercially available dc voltage source and an in-house developed inverter are used in many cases to perform experiments (i.e. [5, 6]). However, the multi-stage conversion circuit of a commercial dc voltage source is too expensive to be installed in an industrial WPT system. Therefore, a single-stage active rectifier including power factor correction, as implemented in [7] for 3 kW, would be a more realistic test environment. This way, interactions between inverter and rectifier can be studied.
This paper therefore deals with the development of an inductive WPT converter operating at 50 Hz three-phase voltage supply at the input and providing a square-wave voltage at the output. First, we describe the components of the power section required for this purpose. The output voltages and currents, as well as the possibility to perform endurance tests, lead to high demands on the safety mechanisms of the converter. In addition, the data acquisition, the analog signal processing and the software of the inverter are covered. Work on this converter was started several years ago (see [8, 9]). Since then, modifications have been made repeatedly to improve the concept. Design considerations regarding best practice experience will be addressed in the last section of the paper.

2 Converter Concept

The design of the converter can be divided into three levels: Software, analog electronics and power section. Fig. 1 shows the conceptual structure with the most important subcomponents of the converter. A computer is responsible for status display, parameter setting and recording of measurement data. It

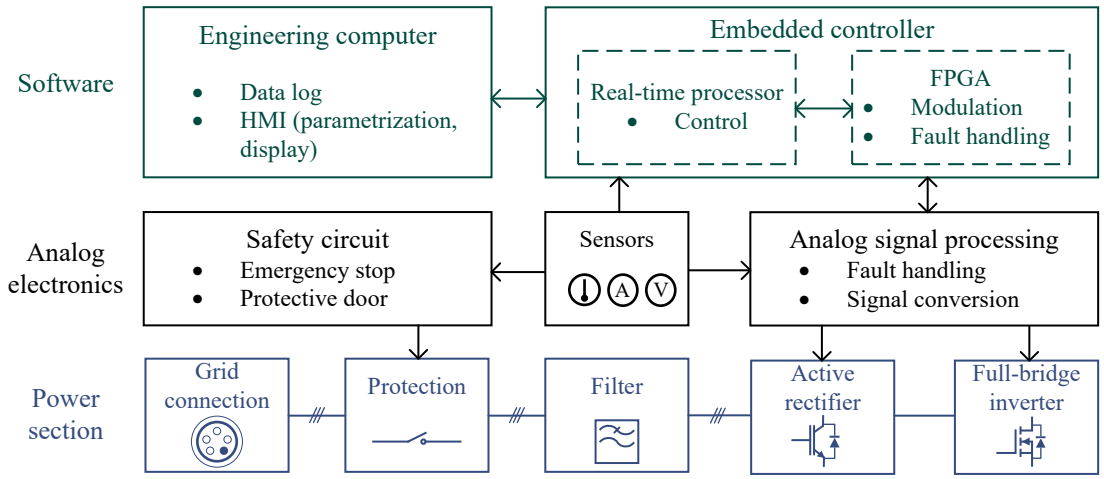

Figure 1: Simplified overview of the converter components.

is connected to the embedded controller via Ethernet. The controller is responsible for control and modulation, as well as fault handling. It receives measurement signals and outputs switching signals.
There are two separate analog safety mechanisms. A safety relay [10] operates in dependence of the dc-link voltage, the cabinet door, the emergency stop buttons and the pre-charging circuit. It can disconnect the supply voltage via a contactor. In addition, the measured values are used to check the voltage, current and temperature of the semiconductors. If a predefined limit is crossed, an analog circuit cuts off the switching signals and deactivates the power electronics.
Fig. 2 shows a photograph of the converter cabinet. The cabinet is completely enclosed, can be moved by means of rollers and, in addition to its use in inductive power transmission, can also be used flexibly as a square-wave voltage source.
In the cabinet, the control unit is located as a separate 19-inch rack module at the very top to minimize electromagnetic interference (EMI) from the power semiconductors positioned below. The protection components are also located in the upper section, behind the control elements.

2.1 Power Section

The power section contains protection elements, EMI filter, rectifier and inverter. It is designed in such a way that the three-phase rectifier cannot be activated until the dc-link has been pre-charged. Fig. 3 shows the equivalent circuit diagram. The rectifier IGBTs are protected with 80 A fuses. Two redundant contactors can interrupt the voltage supply to the active rectifier. One of the contactors has an additional tap, with which the dc-link can be pre-charged internally via an uncontrolled diode rectifier between two phases before active operation. An EMI filter reduces the emission of high-frequency harmonics into the power system. The current smoothing, which is necessary for the operation of the active rectifier, is provided by chokes with an inductance of 500 μH each.
The active rectifier is a self-commutated three-phase bridge circuit equipped with IGBTs [11]. It combines a controllable dc-link voltage with low mains feedback. The semiconductors each have snubber capacitors on the dc side to keep a low inductance of the dc-link connection. The large dc-link capacitance of 2 mF smoothes the voltage. The semiconductors and capacitors can withstand a voltage of 1.7 kV. The diodes of the pre-charging circuit have a breakdown voltage of 1.3 kV [12]. This is unproblematic, since the defect of a diode would hardly cause any costs and the pre-charging resistors limit the short-circuit current. An additional fuse serves to protect the connected components in the event of a short circuit at across the inverter output terminals.
Since no further dc converters are used, the dc-link voltage V_d cannot be reduced below the amplitude of the line voltage:

$$V_\mathrm{d} \geq \sqrt{2} \cdot V_\mathrm{AB}\,. \tag{1}$$

To lower the dc-link voltage, the three-phase voltage must be lowered, for example with the aid of a transformer.

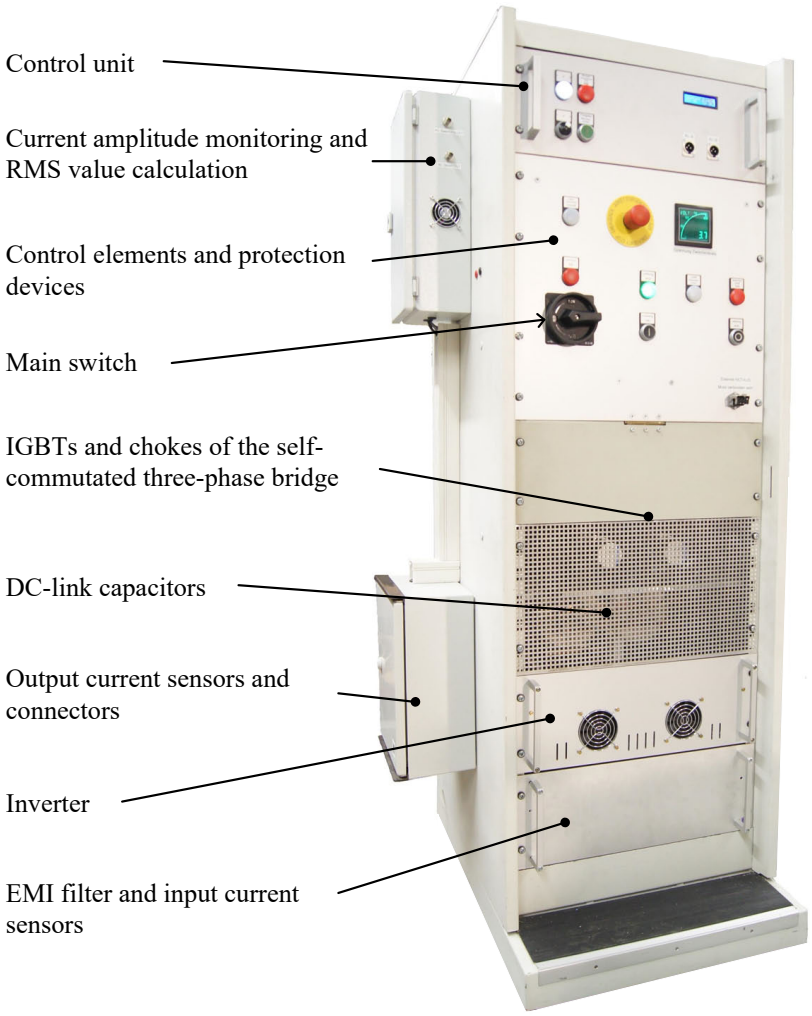

Figure 2: Photograph of the converter cabinet.

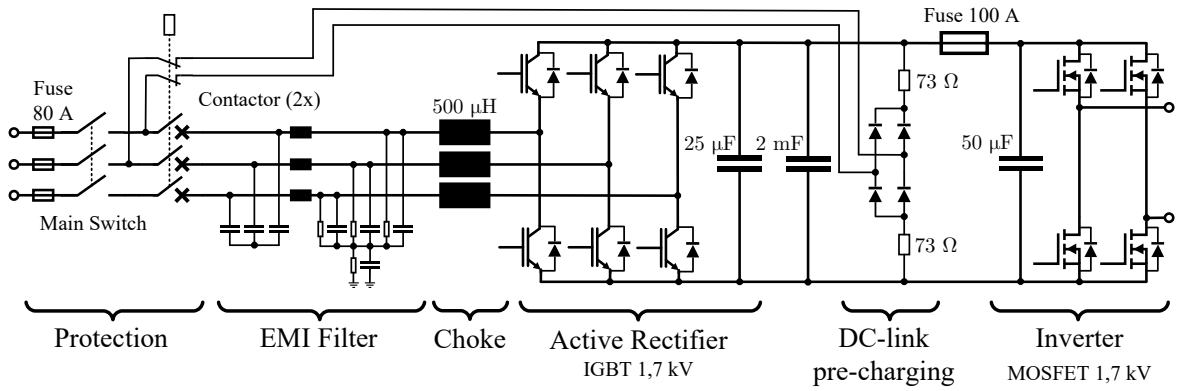

Figure 3: Equivalent circuit diagram of the power section.

The inverter is a self-commutated full-bridge equipped with silicon carbide (SiC) MOSFETs [13]. Due to high frequency operation, square wave modulation (SWM) is used, where each MOSFET turns on and off once each period. It is possible to adjust the first harmonic of the output voltage by symmetrical phase shift (PS) of the inverter half-bridges [14].
The installation of the power electronics in the control cabinet is shown as a CAD model in Fig. 4, as photography is not possible from this perspective. The power semiconductors are mounted on actively

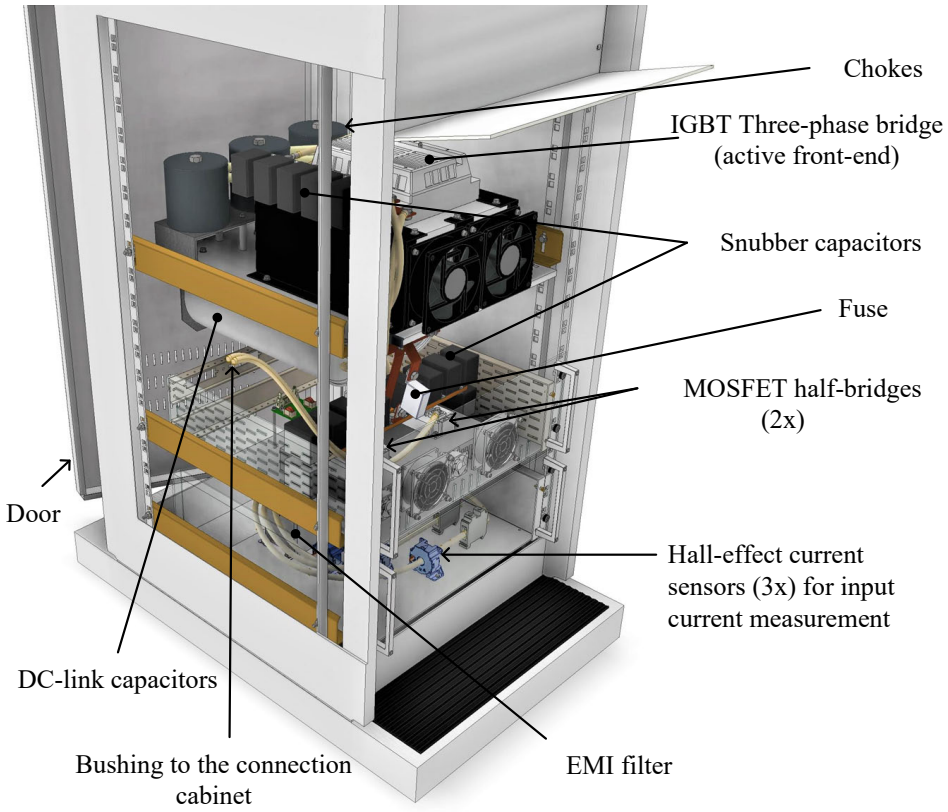

Figure 4: CAD model of the power section in the lower half of the inverter cabinet. The side panel and parts of the front panels have been removed or shown transparently.

cooled heat sinks. The snubber capacitors are located on the dc connections of IGBTs and MOSFETs. The large dc-link capacitors hang below the mounting plate on which the heatsink of the three-phase bridge is installed. Copper bus bars and cables connect the individual components together, with litz wire used at the output of the inverter. The protection technology is not included in this image detail.
For laboratory operation, the semiconductors and the dc-link in particular have been overdimensioned so that there is no danger of destroying them during test phases, even in the event of an emergency shutdown.

2.2 Analog Signal Processing

An overview of the measured values that are acquired and processed within the converter can be found in Fig. 5. In series to the smoothing reactors of the three phases are the current transducers for current measurement also shown in Fig. 4 [15]. These sensors provide a much clearer signal than the integrated current measurement of the self-commutated three-phase bridge. An analog input module of the embedded controller is used to measure the three-phase voltage [16]. This is required to operate the self-commutated three-phase bridge as an active rectifier. The temperature of the IGBTs and MOSFETs, the dc-link voltage and the amplitude of the output current are passed on to the controller and are also checked by an analog enable circuit. Limit value violations lead to the interruption of the switching signals of the respective module.
The determination of the current amplitude and the calculation of the RMS value is done with the analog circuit described in [8, 9]. This is the only measured value of the converter within the high-frequency network. To measure the current waveform with the embedded controller, the measurement signal would have to be passed through the control cabinet and sampled at the controller. The sampling rate would have to be significantly higher than the maximum operating frequency in order to reliably detect limit violations. In [8], however, an analog circuit is implemented that performs a limit value comparison of

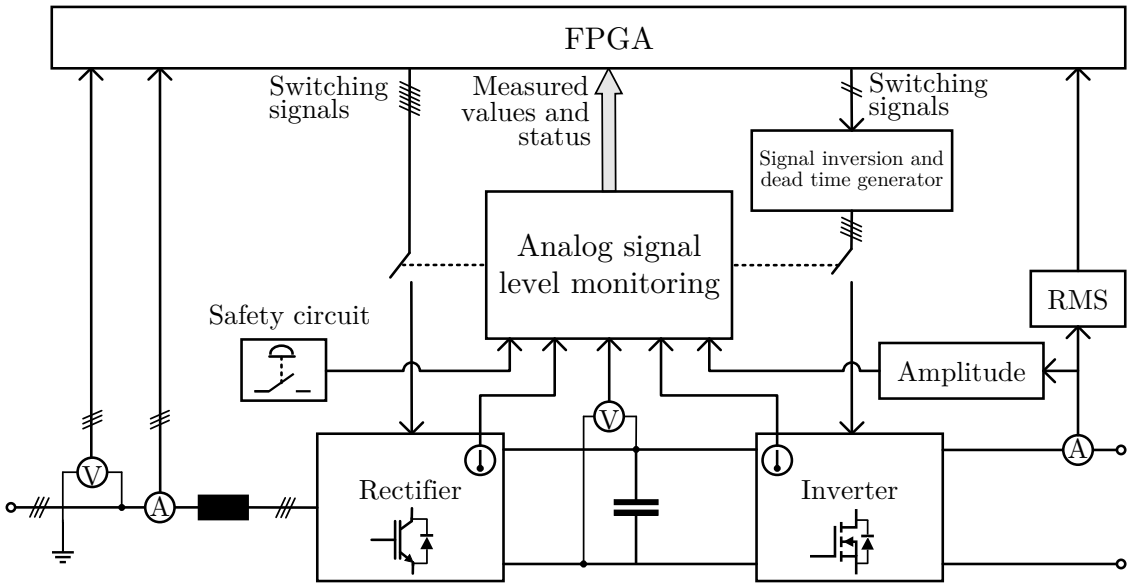

Figure 5: Measured value acquisition in the inverter control cabinet and forwarding to the FPGA of the embedded controller. The switching signals are only passed on to the drivers of the power transistors when enabled.

the current magnitude. The error signal in case of limit exceedance is transmitted to the signal conversion board by optical fibers. Additionally, the circuit outputs a current signal proportional to the RMS value of the current.
The six switching signals from the active rectifier are passed directly to the six IGBT drivers. For the inverter, however, the FPGA outputs only one signal per half-bridge. The MOSFETs of a half-bridge become alternately conductive by generating an inverted signal with dead time, preventing a bridge short circuit.
Fig. 6 shows the control unit as a 19-inch rack module. The circuit board (PCB) contains the analog limit

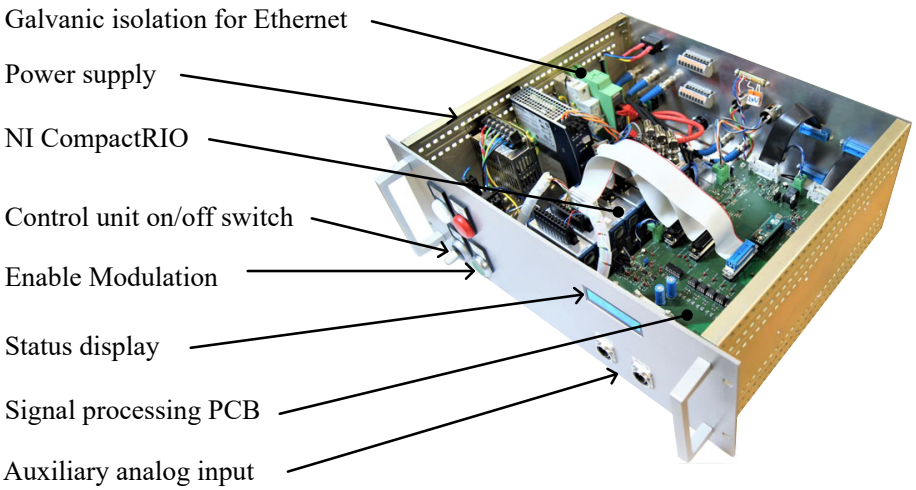

Figure 6: Photograph of the control unit.

value monitoring and the signal processing from Fig. 5, which also includes several analog filters. The embedded controller (NI cRIO) is connected to the board via ribbon cables. The numerous connections of the control unit are located on the front and rear panels. A display gives status information via an additional microcontroller.

2.3 Software

The NI Compact RIO comprises a real-time processor and a Field Programmable Gate Array (FPGA). The programming is done with Labview. Of course, any other type of controller is feasible.

As shown in Fig. 7, the control loops execute on the real-time processor. The active front-end needs

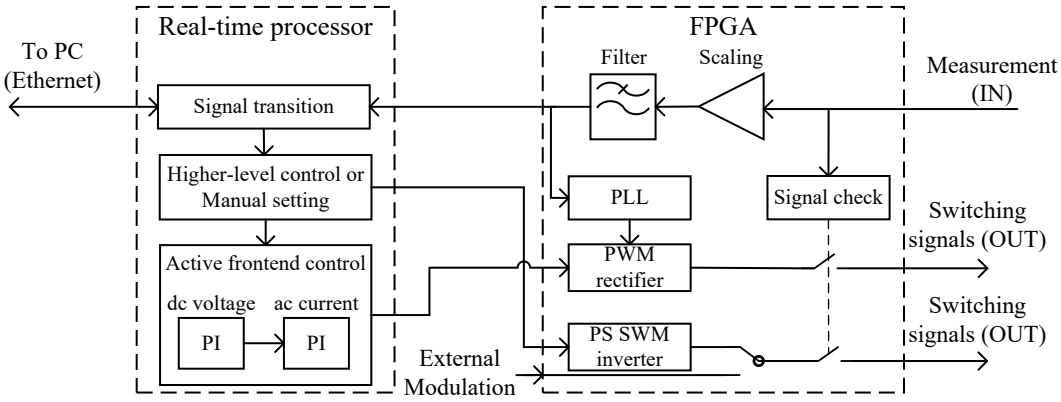

Figure 7: Important functions of the software on the real-time processor and the FPGA.

ac current and dc voltage control loops, which are implemented according to the literature [17, 18]. On a higher level, a custom control scheme can be implemented that affects frequency, half-bridge PS, and dc-link voltage setpoint. Alternatively, a manual setting is possible by means of entering setpoints on the PC. On the FPGA, the phase-locked loop (PLL) and the modulation are implemented. The three-phase bridge is controlled with pulse-width modulation (PWM), and the full bridge inverter is controlled with phase-shift square-wave modulation (PS SWM). The switching signals are only generated if the measured values are within the permissible ranges. In order to be able to use the inverter independently of a computer, an additional digital input is available for direct modulation of the inverter. This is useful for debugging and for quickly integrating the converter into different experimental setups.
The scaling and filtering of measured values would not have to be implemented on the FPGA, but for a clear program structure this division is helpful, since the numerical values of the variables used then have a physical reference. Where further scaling is required for the visualization, signal conversion is performed on the computer.

2.4 Protection

The power section, the analog signal processing PCB and the FPGA each contain protection mechanisms. Table 1 shows the protection response in case of different events. The FPGA handles the most important

Table 1: Overview of the protection mechanisms

Event	**FPGA disables switching signals**	**Analog circuit disables switching signals**	**Contac-tor opens**	**Fuse trips**
DC link voltage is too high	X	X	X	
DC link voltage is too low	X			
AC supply current is too high	X			X
Inverter output current is too high		X		X
Heat sink temperature is too high	X	X		
Door opens or emergency stop button is pressed		X	X	
User triggers emergency stop in the HMI	X			
Auxiliary power supply fails	X	X	X	

safety functions of the inverter, since it has the shortest response time of approximately 1 μs for disabling the switching signals. The analog signal monitoring interrupts the switching signals about 10 ms after

detection of a fault condition. The contactor requires 15 ms opening time. The fuses only trip if other protective measures failed. Here, the 100 A fuse on the dc-busbar is responsible for disconnecting the inverter output from the dc-link. The MOSFETs can conduct more current, but the internal wiring is only rated for 100 A. The 80 A fuses at the ac input will trip if the input current is too high.
The analog safety circuit and the safety relay are normally open, so that the switching signals are cut off without auxiliary power supply.

3 Operating Performance

The converter has been tested with an output power of up to 24 kW. Fig. 8 shows the voltage curve at two different phase angles. In addition to the influence of the frequency, the dc-link voltage and phase-shift,

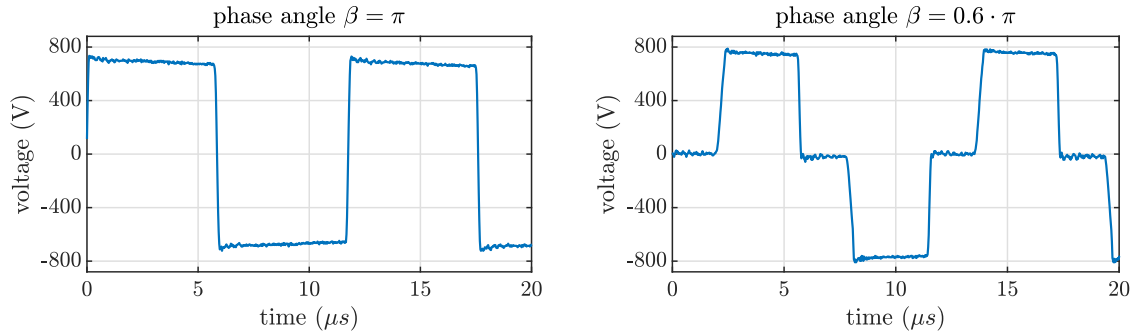

Figure 8: Measured output voltage curves of the inverter with ZVS at different phase angles.

the current curve also affects the voltage waveform. If zero voltage switching (ZVS) is achieved due to a lagging current, there is hardly any overshooting of the voltage. The current itself depends on the connected load network. The voltage gradient is also dependent on the output current. For soft switching in Fig. 8, it is about $2\,\mathrm{kV}/\mu\mathrm{s}$. Without ZVS, about $20\,\mathrm{kV}/\mu\mathrm{s}$ can be reached.
When operating on 400 V mains, the dc-link voltage can be varied between 580 V and 1000 V. To set lower voltages, the supply voltage must be reduced. The converter is functional from 24 V line voltage, so that the minimum dc-link voltage is 34 V.

4 Practical Design Considerations

This section describes the experience gained from installing and operating the converter.

4.1 Modular Design

When designing the converter, particular attention was paid to the fact that individual units can be exchanged independently to accommodate changing requirements. Both the power semiconductors and the control unit are structured in 19-inch rack modules. Within the control unit, the cRIO can be easily expanded by additional plug-in modules.

4.2 Electromagnetic Interference

With high-frequency switching operations of up to 1000 V, EMI is inevitably a relevant issue. During the design of the converter, attention was already paid to high interference immunity. The control unit is a closed, grounded cabinet with the greatest possible distance to the power semiconductors. Signal lines in the converter cabinet are shielded. However, the digital switching signals within the control unit can also cause interference on analog signals. Measurement signals should therefore also be transmitted shielded within the control unit.
Fig. 9 shows the signal of a magnetoresistive (MR) current sensor. Measuring the output current of the inverter, the MR sensor is connected to one MOSFET half-bridge and can therefore not be shielded against its transient emissions. As its signal is interfered even though the MOSFETs switch softly in Fig. 9, it had to be replaced by a current transducer.
Hard switching may occur during test operation of new coil systems or control concepts for inductive charging. The power electronics therefore are dimensioned such that hard switching will not cause any harm. However, hard switching implies ringing as shown in Fig. 9. The output cables act as an antenna

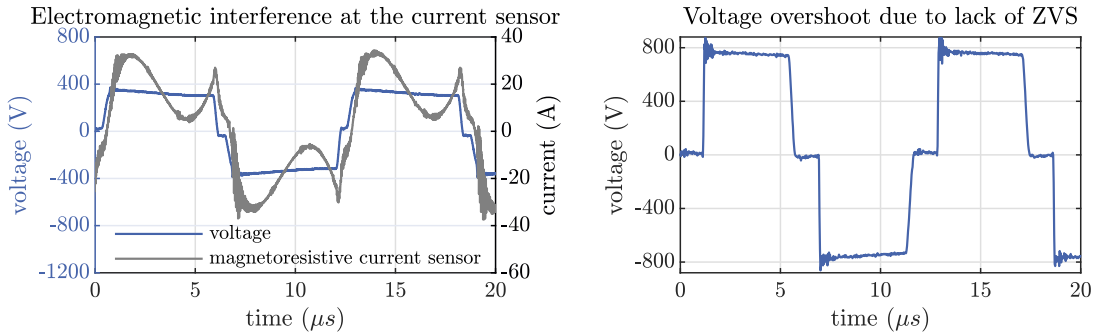

Figure 9: Practical challenges: EMI at a magnetoresistive current sensor and ringing due to lack of ZVS.

for high-frequency EMI [19]. As a result, nearby devices like a display, oscilloscope or keyboard were disturbed during tests when ZVS could not be achieved.

4.3 Startup and Shutdown Process

To avoid hard switching and subsequent EMI problems it is essential to plan the startup and shutdown process of the inverter. ZVS can only be achieved in a steady-state oscillating system. Therefore, the switching signals of both half-bridges must begin and end exactly synchronously and changes of the operating point must be smoothly executed. The contact bounce of mechanical relays, as used in common signal generators, prohibits their application to enable the switching signals. The most feasible starting process in this case is enabling all switching signals in a single cycle of the embedded controllers FPGA. The shutdown can be implemented likewise.

5 Conclusion

This publication describes the development, design and implementation of a converter that can be used to generate a square-wave voltage for testing inductive power transmission systems. The converter is supplied from the three-phase low-voltage grid. It has the simplest possible design that can realize dc-link voltage control, consisting of a self-commutated three-phase bridge as a rectifier and a single-phase full-bridge inverter. The power electronic circuit, key components, and the construction are described. In addition to the functionality of the converter, the avoidance of EMI and the safety technology have special priority. For switching operations with up to 1000 V dc-link voltage, ZVS is necessary to avoid interference with other devices. For this purpose, it must also be possible to activate and deactivate the switching signals fully synchronously.

References

[1] Hybrid - EV Committee, “Wireless power transfer for light-duty plug-in/electric vehicles and alignment methodology,” Warrendale, PA, United States, 2020.

[2] A. P. Hu, *Wireless/contactless power supply: Inductively coupled resonant converter solutions*. Saarbrücken: VDM Verlag Dr. Müller, 2009.

[3] M. Maier, D. Maier, M. Zimmer, and N. Parspour, “A novel self oscillating power electronics for contactless energy transfer and frequency shift keying modulation,” in *2016 International Symposium on Power Electronics, Electrical Drives, Automation and Motion (SPEEDAM)*. IEEE, 2016, pp. 67–72.

[4] S. Assawaworrarit, X. Yu, and S. Fan, “Robust wireless power transfer using a nonlinear parity-time-symmetric circuit,” *Nature*, vol. 546, no. 7658, pp. 387–390, 2017.

[5] J. Colussi, A. La Ganga, R. Re, P. Guglielmi, and E. Armando, “100 kw three-phase wireless charger for ev: Experimental validation adopting opposition method,” *Energies*, vol. 14, no. 8, p. 2113, 2021. [Online]. Available: https://www.mdpi.com/1996-1073/14/8/2113

[6] R. Bosshard, U. Iruretagoyena, and J. W. Kolar, “Comprehensive evaluation of rectangular and double-d coil geometry for 50 kw/85 khz ipt system,” *IEEE Journal of Emerging and Selected Topics in Power Electronics*, vol. 4, no. 4, pp. 1406–1415, 2016.

[7] C. Joffe, S. Ditze, and A. Rosskopf, "A novel positioning tolerant inductive power transfer system," in *2013 3rd International Electric Drives Production Conference (EDPC)*. IEEE, 29.10.2013 - 30.10.2013, pp. 1–7.

[8] B. Klaus, B. Muller, M. Sack, and T. Leibfried, "Contactless electric vehicle charging - development of a high power resonance converter: Special features during design process for an experimental setup," in *2015 IEEE Vehicle Power and Propulsion Conference (VPPC)*. Piscataway, NJ: IEEE, 2015, pp. 1–6.

[9] B. Klaus, D. Barth, D. Woll, and T. Leibfried, "Development and construction of a measurement device for testing and safe operation of experimental wireless electric vehicle chargers," in *2017 IEEE 12th International Conference on Power Electronics and Drive Systems (IEEE PEDS 2017)*. Piscataway, NJ: IEEE, 2017, pp. 287–290.

[10] Eaton Industries GmbH, "Esr5-no-31-230vac: Safety relay emergency stop/protective door, 230vac, 3 enabling paths," 2022. [Online]. Available: https://datasheet.eaton.com/datasheet.php?model=119380

[11] SEMIKRON International GmbH, "Skiip 292gd170-3du: 6-pack - integrated intelligent power system," 2007.

[12] Vishay Intertechnology, Inc., "By255p: General purpose plastic rectifier," 2013. [Online]. Available: https://www.vishay.com/docs/88838/by251p.pdf

[13] Cree Inc., "Cas300m17bm2: All-silicon carbide half-bridge module," Durham, NC 27703, 2018. [Online]. Available: https://assets.wolfspeed.com/uploads/2020/12/cas300m17bm2.pdf

[14] G. Lovison, T. Imura, H. Fujimoto, and Y. Hori, "Secondary-side-only control for smooth voltage stabilization in wireless power transfer systems with constant power load," in *2018 International Power Electronics Conference (IPEC-Niigata 2018 -ECCE Asia)*. IEEE, 2018, pp. 77–83.

[15] LEM International SA, "Current transducer lf 210-s/sp5," Switzerland, 2021. [Online]. Available: https://www.lem.com/en/lf-210ssp5

[16] National Instruments, "Ni 9242 datasheet," 2016. [Online]. Available: www.ni.com

[17] F. Liccardo, P. Marino, and M. Triggianese, "Design criteria for a synchronous active front-end in high power applications," in *International Symposium on Power Electronics, Electrical Drives, Automation and Motion, 2006. SPEEDAM 2006*. IEEE, 2006, pp. 1252–1257.

[18] H. V. Luu, A. Punzet, V. Muller, and N. L. Phung, "Control of front-end converter with shunt active filter using adaptive gain," in *2005 European Conference on Power Electronics and Applications*. IEEE, 2005, pp. 10 pp–P.10.

[19] P. Deng, B. Zhou, S. Li, X. Qing, Z. Liu, and C. Tang, "Modeling and analysis of emi of full-bridge inverter for lcc-s compensated wpt system," in *2020 8th International Conference on Power Electronics Systems and Applications (PESA)*, 2020, pp. 1–5.

Presenter Biography

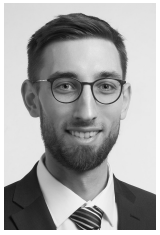

Daniel Barth was born in Bad Soden am Taunus, Germany, in 1990. He received the M.Sc. degree in electrical engineering from the Karlsruhe Institute of Technology, Karlsruhe, Germany, in 2015, where he is currently working towards the PhD degree in electrical engineering. His research interests include high-power wireless charging of electric vehicles, magnetic path control, magnetic field modeling, and the characterization of materials for wireless power transfer.

Johannes Scholl was born in Neuwied, Germany, in 1996. He received the B.Sc. degree in electrical engineering from the Karlsruhe Institute of Technology, Karlsruhe, Germany, in 2021, where he is currently studying for the M.Sc. degree in electrical engineering with a focus on electrical machines and power electronics.

Erik Wöhr was born in Pforzheim, Germany, in 1997. He received his B.Sc. degree in electrical engineering from the Karlsruhe Institute of Technology, Karlsruhe, Germany, in 2020, where he is currently studying for the M.Sc. degree in electrical engineering.

Michael Suriyah was born in Kuala Lumpur, Malaysia, in 1982. He received the Diploma and M.Sc. degrees in electrical engineering from the University of Applied Sciences, Karlsruhe, Germany, in 2007 and 2008, respectively, and the Ph.D. degree in electrical engineering from KIT, Karlsruhe, in 2013. He is the Head of the Department for Power Networks with the Institute of Electric Energy Systems and High-Voltage Technology. His research interests include aging diagnostics and onsite testing of power transformers, high-voltage testing methods, analysis of electric power networks as well as planning of future power systems. He is a member of VDE.

Thomas Leibfried was born in Neckarsulm, Germany, in 1964. He received the Dipl.Ing. and Dr. Ing. degrees from the University of Stuttgart, Stuttgart, Germany, in 1990 and 1996, respectively. From 1996 to 2002, he was with Siemens AG, Nuremberg, Germany, working in the power transformer business in various technical and management positions. In 2002, he joined the University of Karlsruhe, Karlsruhe, Germany, as the Head of the Institute of Electric Energy Systems and High-Voltage Technology. He is a member of VDE and CIGRE.